



CrossMark
click for updates

Cite this: *RSC Adv.*, 2016, 6, 91981

Tailored honeycomb-like polymeric films based on amphiphilic poly(urea/malonamide) dendrons†

Chien-Hsin Wu,^a Wei-Ho Ting,^b Yu-Wen Lai,^a Shenghong A. Dai,^b Wen-Chiung Su,^c Shih-Huang Tung^{*a} and Ru-Jong Jeng^{*a}

A series of hydrogen bond-rich poly(urea/malonamide) dendrons were utilized as surfactants to facilitate the formation of honeycomb-like porous structures from the breath figure (BF) process. With the addition of a small amount of dendritic surfactants to polymers such as poly(D,L-lactide), polystyrene or poly(methyl methacrylate), a well-organized honeycomb-like surface could be achieved. These uniform porous arrays from the BF method with free-standing capacity benefit from the support of their polymer matrices without resorting to a painstaking polymerization process to provide bulky dendritic side-chain polymers. The formation of water-driven honeycomb-like surfaces was also dependent on the concentration of surfactants in a polymer matrix, apart from the chemical structure. Furthermore, a quantitative analysis of the interfacial tensions between water and polymer solution revealed a dynamic procedure of water droplets stabilized by the surfactants on the as-cast polymer films during the solvent evaporation step of the BF method. Among all these dendritic surfactants, the dendrons with one or two hydroxyl groups at the focal point and plenty of octadecyl groups in the periphery exhibited an amphiphilic nature, and were able to create well-balanced interfacial tensions capable of maintaining water in droplets. Consequently, this type of dendron as a surfactant can be blended with a wide range of polymers to create regular honeycomb-like arrays.

Received 16th June 2016
Accepted 14th September 2016

DOI: 10.1039/c6ra15636c

www.rsc.org/advances

1. Introduction

The breath figure (BF) method is an easy process to fabricate well-organized honeycomb-like polymeric films.¹ In this method, a polymer solution dissolved in volatile solvents such as chloroform (CHCl₃) or carbon disulfide (CS₂) is cast on a substrate under highly humid air. Subsequently, the water droplets from saturated vapor condense on the cooling surface owing to the evaporation of solvent in the polymer solution. The growing droplets packed into a hexagonal array can be used as templates to make honeycomb-like patterns on the polymer surface after complete evaporation of solvent and water.^{2–5} Due to their versatility, honeycomb-like films from BF have drawn much interest in a variety of applications, such as biofilm suppression,⁶ anti-reflection coatings,⁷ vapor sensors,⁸ cell growth scaffolds,⁹ superhydrophobic surfaces,¹⁰ and microsieves.¹¹

The stabilization between water droplets and polymer solution is crucial for creating the uniform array of water droplets that is necessary for the formation of honeycomb-like films

from the BF method. However, for ordinary linear polymers such as polylactide (PLA) with hydrophobic ester functional groups, it is difficult to stabilize the water droplets in most cases.⁴ To overcome this restriction, several studies have reported that surfactants or block copolymers can be added to the polymer solution to assist the formation of honeycomb-like films.^{12–20} These amphiphilic additives locating at the interface between the water droplets and the polymer solution are intended to facilitate the condensation of water vapor while preventing water droplets aggregating further. Therefore, the surfactants would be water-insoluble molecules with sufficient hydrophobic segments and polar head groups to adsorb onto the surface of the polymer solution.²¹ Shimomura *et al.* used an interfacial tension method to investigate surfactant ability during the formation of honeycomb-like films from the BF method, and found that the stability of water droplets is highly dependent on the concentration and structure of surfactants.²²

Dendritic polymers are known for their dense functional groups and monodispersity, making them good candidates for ordered self-assembly.²³ Recently, we developed new types of dendritic poly(urea/malonamide) polymers *via* a convergent route and their self-assembly behaviors have been studied.^{24–30} These dendrons are amphiphilic, with a hydrogen-bond-rich focal part and a periphery with nonpolar units that undergo van der Waals interactions. These dendrons were grafted onto either nonpolar or polar polymer backbones, including

^aInstitute of Polymer Science and Engineering, National Taiwan University, Taipei 106, Taiwan. E-mail: rujong@ntu.edu.tw

^bDepartment of Chemical Engineering, National Chung Hsing University, Taichung 402, Taiwan

^cNational Chung Shan Institute of Science and Technology, Taoyuan 325, Taiwan

† Electronic supplementary information (ESI) available: Supplementary figures. See DOI: 10.1039/c6ra15636c

polystyrene (PS) and polyurethane (PU) based polymers, to prepare porous films by the BF method.^{31–33} Using this approach, we were able to create superhydrophobic polymer surfaces.

It is important to note that the poly(urea/malonamide) dendrons were capable of yielding honeycomb-like films by unconventional BF processes through supramolecular aggregates, as shown by the examples of several organic molecules.³⁴ Nevertheless, the purpose of this study focuses on the direct use of the poly(urea/malonamide) dendrons as surfactants without grafting them onto the polymer backbone. Instead of resorting to complicated chemical synthesis, the poly(urea/malonamide) dendrons were simply blended with common polymers, such as poly(D,L-lactide) (PLA), PS, polycarbonate (PC), poly(methyl methacrylate) (PMMA), or polycaprolactone (PCL), to prepare porous films from polymer solutions by the BF method. The dendrons of different generations with hydroxyl functional groups in the focal part ($-\text{N}(\text{CH}_2\text{CH}_2\text{OH})_2$, $-\text{CH}_2\text{CH}_2\text{OH}$, and $-\text{CH}_2\text{CH}_2\text{CH}_2\text{CH}_3$) and the peripheral hydrophobic part ($-\text{C}18$ and $-\text{C}4$) were synthesized to assist the formation of a honeycomb-like structure. Polymer films with highly ordered honeycomb micropores were achieved with the addition of dendritic surfactants. The dependence of the honeycomb-like structures from the BF method on the concentration and structure of dendritic surfactants was investigated. The interfacial tensions of the dendron/polymer solutions were measured through the ring method, and correlated with the morphology of the honeycomb-like structure.

2. Experimental

Materials

Methylene di-*p*-phenyl diisocyanate (MDI), isobutyl chloride, triethylamine, 1-octadecanol, *n*-butanol, *N*-(3-aminopropyl) diethanolamine (APDEA), ethanolamine (ETA), *n*-butylamine, PLA (M_w 75 000–120 000), PS ($M_w \sim 192$ 000), PC ($M_w \sim 45$ 000), PMMA ($M_w \sim 45$ 000), and PCL ($M_n \sim 80$ 000) were all reagent grade purchased from Acros, Sigma-Aldrich, TEDIA, TCI and SHOWA. Xylene, tetrahydrofuran (THF), trichloromethane (chloroform) and cyclohexane were distilled under reduced pressure over MgSO_4 or CaH_2 and stored over 4 Å molecular sieves. Other reagents were used as received without further purification.

Synthesis of dendritic poly(urea/malonamide)

In Scheme 1, the dendritic poly(urea/malonamides) with alkyl chains comprising 18 carbons (G0.5-C18, G1.5-C18 and G2.5-C18) based on a building block, 4-isocyanate-4'-(3,3-dimethyl-2,4-dioxo-azetidine)diphenyl methane (IDD), were synthesized according to procedures described in our previous works.^{35,36} Furthermore, the general procedure for making dendritic poly(urea/malonamides) with butyl groups in the periphery (G0.5-C4, G1.5-C4 and G2.5-C4) were followed as described below.

G0.5-C4. A solution of IDD (6 g, 18.75 mmol) in dry THF (40 mL) was mixed with *n*-butanol (1.39 g, 18.75 mmol) at 70 °C

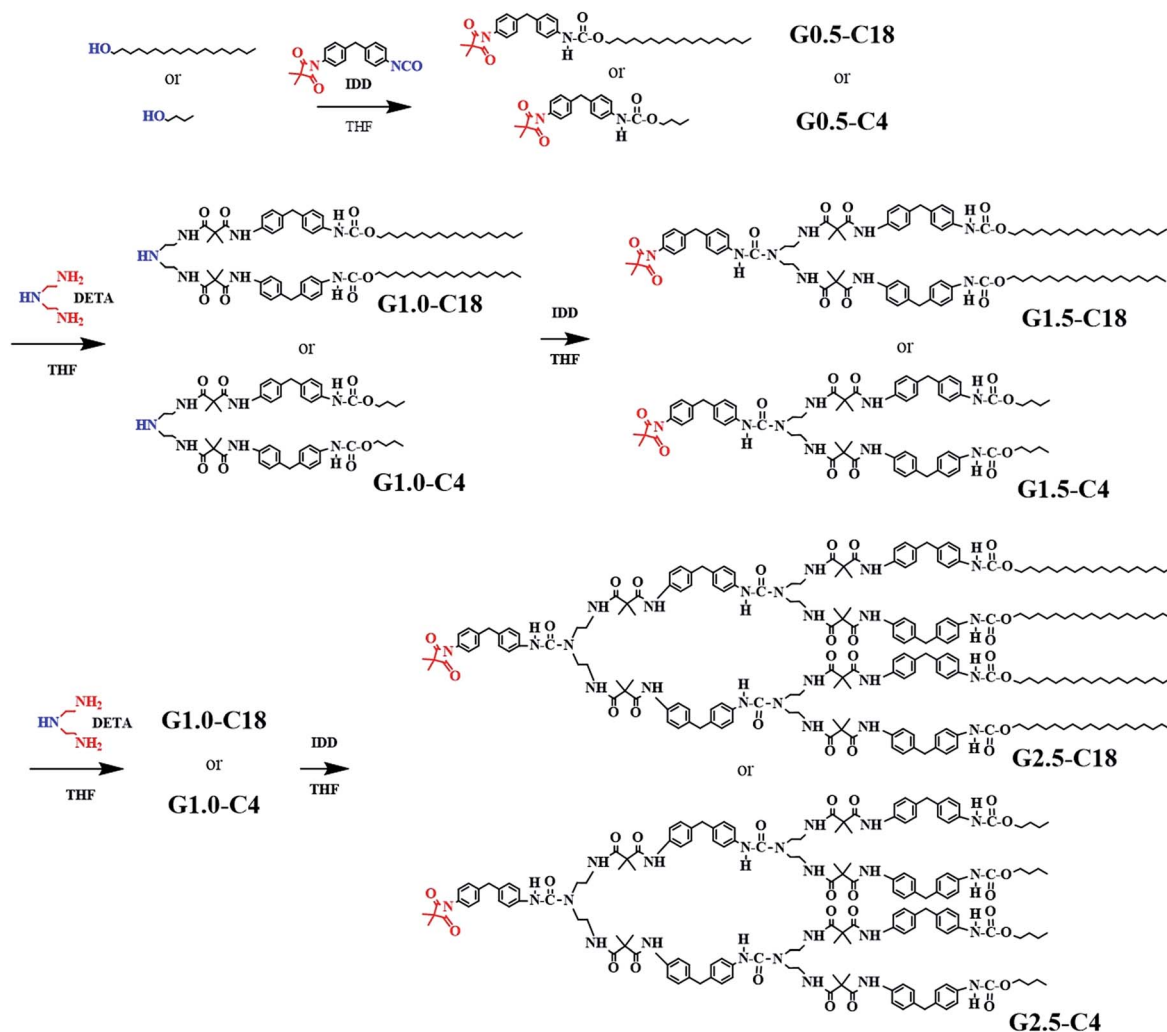
under dry N_2 for 4 h. The mixture was purified by silica gel chromatography with EA/*n*-hexane = 2/1 to obtain G0.5-C4 as white powder. FT-IR (KBr): 3338 cm^{-1} (NH), 1857 cm^{-1} (C=O), 1734 cm^{-1} (C=O). ^1H NMR (chloroform-*d*): δ (ppm) = 0.92 (3H, t, CH_3), 1.40 (2H, m, CH_2), 1.45 (6H, s, CH_3), 1.63 (2H, m, CH_2), 3.90 (2H, s, Ar- CH_2 -Ar), 4.13 (2H, t, CH_2), 7.05–7.72 (8H, m, Ar-H). Elemental analysis ($\text{C}_{23}\text{H}_{26}\text{N}_2\text{O}_4$): calcd: C 70.03, H 6.64, N 7.10; found: C 70.06, H 6.62, N 7.09. MS (LC-MS): m/z = 394.1 (M^+). GPC (THF): PDI = 1.00, M_n = 514, M_w = 517.

G1.0-C4. A solution of DETA (0.60 g, 6.0 mmol) was added to a solution of G0.5-C4 (5 g, 12.7 mmol) in dry THF (25 mL) at 70 °C under dry N_2 . After 4 h, all of the DETA was consumed. Subsequently, the mixture was purified by silica gel chromatography with EA to obtain G1.0-C4 (4.5 g, 84%) as a white powder. FT-IR (KBr): 3355 cm^{-1} (NH), 1707 cm^{-1} [(NH)C=O]. ^1H NMR (chloroform-*d*): δ (ppm) = 0.95 (6H, t, CH_3), 1.40 (4H, m, CH_2), 1.51 (12H, s, CH_3), 1.63 (4H, m, CH_2), 2.70 (4H, t, CH_2), 3.27 (4H, t, CH_2), 3.90 (4H, s, Ar- CH_2 -Ar), 4.12 (4H, t, CH_2), 7.05–7.42 (16H, m, Ar-H). Elemental analysis ($\text{C}_{50}\text{H}_{65}\text{N}_7\text{O}_8$): calcd: C 67.32; H 7.34; N 10.99; found: C 67.18; H 7.19; N 10.79. MS (LC-MS): m/z = 891.6 (M^+). GPC (THF): PDI = 1.01, M_n = 933, M_w = 943.

G1.5-C4. A solution of IDD (2.24 g, 7.0 mmol) in dry THF (40 mL) was mixed with G1.0-C4 (5.0 g, 5.6 mmol) at 60 °C under dry N_2 . After 4 h, all of the G-1.0-C4 was consumed, as monitored through a TLC test. The mixture was purified by silica gel chromatography with EA to obtain G1.5-C4 (4.5 g, 84%) as a white powder. FT-IR (KBr): 3320 cm^{-1} (NH), 1853 cm^{-1} (C=O), 1754 cm^{-1} (C=O). ^1H NMR (chloroform-*d*): δ (ppm) = 0.98 (6H, t, CH_3), 1.40 (4H, m, CH_2), 1.46 (6H, s, CH_3), 1.52 (12H, s, CH_3), 1.65 (4H, m, CH_2), 3.38 (8H, t, CH_2), 3.84–3.90 (6H, s, Ar- CH_2 -Ar), 4.12 (4H, t, CH_2), 7.03–7.92 (24H, m, Ar-H). Elemental analysis ($\text{C}_{69}\text{H}_{81}\text{N}_9\text{O}_{11}$): calcd: C 68.35; H 6.73; N 10.40; found: C 69.01; H 6.73; N 10.91. MS (LC-MS): m/z = 1211.5 (M^+). GPC (THF): PDI = 1.01, M_n = 1911, M_w = 1922.

G2.0-C4. A solution of DETA (0.2 g, 2.0 mmol) was added to a solution of G1.5-C4 (5 g, 4.1 mmol) in dry THF (25 mL) at 60 °C under dry N_2 . After 6 h, all of the DETA was consumed. The mixture was purified by silica gel chromatography with EA to obtain G2.0-C4 (4.0 g, 80%) as a white powder. FT-IR (KBr): 3313 cm^{-1} (NH), 1707 cm^{-1} [(NH)C=O]. ^1H NMR (chloroform-*d*): δ (ppm) = 0.96 (12H, t, CH_3), 1.41 (8H, m, CH_2), 1.51 (36H, s, CH_3), 1.64 (8H, m, CH_2), 2.66 (4H, t, CH_2), 3.25 (20H, m, CH_2), 3.83 (12H, s, Ar- CH_2 -Ar), 4.13 (8H, t, CH_2), 7.06–7.55 (48H, m, Ar-H). Elemental analysis ($\text{C}_{142}\text{H}_{175}\text{N}_{21}\text{O}_{22}$): calcd: C 67.46, H 6.98, N 11.46; found: C 66.87, H 7.13, N 11.10. MS (LC-MS): m/z = 2528.3 (M^+). GPC (THF): PDI = 1.01, M_n = 2692, M_w = 2665.

G2.5-C4. A solution of IDD (0.7 g, 2.19 mmol) in dry THF (25 mL) was mixed with G2.0-C4 (4.6 g, 1.82 mmol) at 60 °C under dry N_2 . After 4 h, all of the G2.0-C4 was consumed, as monitored through a TLC test. The mixture was purified by silica gel chromatography with EA to obtain G2.5-C4 (3.6 g, 70%) as a white powder. FT-IR (KBr): 3292 cm^{-1} (NH), 1832 cm^{-1} (C=O), 1728 cm^{-1} (C=O), 1678 cm^{-1} [(NH)C=O]. ^1H NMR (chloroform-*d*): δ (ppm) = 0.95 (12H, t, CH_3), 1.41 (8H, m, CH_2), 1.46 (6H, s, CH_3), 1.51 (36H, s, CH_3), 1.64 (8H, m, CH_2), 3.25 (24H, m, CH_2), 3.82 (12H, s, Ar- CH_2 -Ar), 3.91 (2H, s, Ar-



Scheme 1 Preparation of poly(urea/malonamide) dendrons.

CH₂-Ar), 4.13 (8H, t, CH₂), 7.06–7.75 (56H, m, Ar-H). Elemental analysis (C₁₆₁H₁₉₁N₂₃O₂₅): calcd: C 67.89, H 6.76, N 11.31; found: C 63.70, H 6.18, N 10.24. MS (LC-MS): *m/z* = 2848.1 (M⁺). GPC (THF): PDI = 1.01, *M_n* = 3066, *M_w* = 3089.

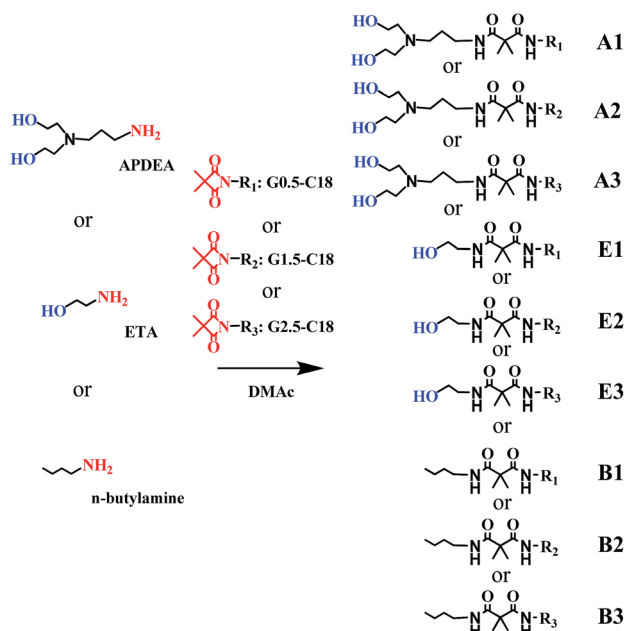
Synthesis of amphiphilic dendrons

The general procedures for preparing poly(urea/malonamides) are described below (Scheme 2). A reactive aztidine-2,4-dione functional group is located at the focal point of the dendrons (G0.5-C18, G1.5-C18, G2.5-C18). Reagents containing a primary amine with various numbers of hydroxyl functional groups (–N(CH₂CH₂OH)₂, –CH₂CH₂OH, and –CH₂CH₂CH₂CH₃) were reacted with poly(urea/malonamide) dendrons to modify their hydrophilicity in the focal point. Among them, compounds A1, A2 and A3 were synthesized in our previous works.^{26,32}

Compound E1. A solution of G0.5-C18 (2.38 g, 4 mmol) in dry THF (15 mL) was mixed with ETA (0.3 g, 4.8 mmol) at 70 °C under dry nitrogen gas. The reaction mixture was stirred for 3 h and all of the G0.5-C18 was consumed as monitored by IR spectra. E1 (2.22 g, 85%) was purified by precipitation from

methanol as a light yellow powder. FT-IR (KBr): 3356 cm⁻¹ (NH), 1707 cm⁻¹ [(NH)C=O]. ¹H NMR (chloroform-d): δ (ppm) = 0.86 (3H, t, CH₃), 1.32 (30H, m, CH₂), 1.53 (6H, s, CH₃), 1.63 (2H, m, CH₂), 3.42 (2H, t, CH₂), 3.70 (2H, t, CH₂), 3.86 (2H, s, Ar-CH₂-Ar), 4.11 (2H, t, CH₂), 7.05–7.42 (8H, m, Ar-H). Elemental analysis (C₃₉H₆₁N₃O₅): calcd: C 71.85, H 9.43, N 6.45; found: C 71.25, H 9.27, N 6.21. MS (LC-MS): *m/z* = 651.5 (M⁺). GPC (THF): PDI = 1.01, *M_n* = 1439, *M_w* = 1452.

Compound E2. A solution of G1.5-C18 (6 g, 3.74 mmol) in dry THF (25 mL) was mixed with ETA (0.27 g, 7.5 mmol) at 70 °C under dry nitrogen gas. The reaction mixture was stirred for 6 h and all of the G1.5-C18 was consumed, as monitored by IR spectra. E2 (3.74 g, 61%) was purified by precipitation from methanol as a light yellow powder. FT-IR (KBr): 3356 cm⁻¹ (NH), 1703 cm⁻¹ [(NH)C=O]. ¹H NMR (chloroform-d): δ (ppm) = 0.86 (6H, t, CH₃), 1.23 (60H, m, CH₂), 1.52 (18H, s, CH₃), 1.61 (4H, m, CH₂), 2.70 (6H, t, CH₂), 3.42 (6H, t, CH₂), 3.82 (6H, s, Ar-CH₂-Ar), 4.11 (4H, t, CH₂), 7.00–7.52 (24H, m, Ar-H). Elemental analysis (C₉₉H₁₄₄N₁₀O₁₂): calcd: C 71.36, H 8.71, N 8.41; found: C 72.60, H 8.28, N 7.90. MS (LC-MS): *m/z* = 1666.9 (M⁺). GPC (THF): PDI = 1.01, *M_n* = 2093, *M_w* = 2115.



Scheme 2 Preparation of amphiphilic poly(urea/malonamide) dendrons.

Compound E3. A solution of G2.5-C18 (6 g, 1.65 mmol) in dry THF (25 mL) was mixed with ETA (0.20 g, 3.30 mmol) at 70 °C under dry nitrogen gas. The reaction mixture was stirred for 6 h and all of the G2.5-C18 was consumed, as monitored by IR spectra. E3 (3.72 g, 61%) was purified by precipitation from methanol as a light yellow powder. FT-IR (KBr): 3356 cm^{-1} (NH), 1707 cm^{-1} [(NH)C=O]. ^1H NMR (DMSO- d_6): δ (ppm) = 0.81 (12H, t, CH_3), 1.20 (120H, m, CH_2), 1.32 (42H, s, CH_3), 1.53 (8H, m, CH_2), 2.55 (14H, t, CH_2), 3.08 (14H, t, CH_2), 3.74 (14H, s, Ar- CH_2 -Ar), 4.01 (8H, t, CH_2), 7.00–7.65 (56H, m, Ar-H). Elemental analysis ($\text{C}_{219}\text{H}_{310}\text{N}_{24}\text{O}_{26}$): calcd: C 71.19; H 8.46; N 9.10; found: C 70.08; H 8.12; N 9.75. MS (MALDI-TOF): m/z = 3692.4 (M^+). GPC (THF): PDI = 1.01, M_n = 4297, M_w = 4334.

Compound B1. A solution of G0.5-C18 (2.95 g, 5 mmol) in dry THF (25 mL) was mixed with *n*-butylamine (0.44 g, 6 mmol) at 70 °C under dry nitrogen gas. The reaction mixture was stirred for 4 h and all of the G0.5-C18 was consumed, as monitored by IR spectra. B1 (2.82 g, 85%) was purified by precipitation from methanol as a light yellow powder. FT-IR (KBr): 3350 cm^{-1} (NH), 1707 cm^{-1} [(NH)C=O]. ^1H NMR (chloroform- d): δ (ppm) = 0.95 (6H, t, CH_3), 1.23 (32H, m, CH_2), 1.47 (2H, m, CH_2), 1.52 (6H, s, CH_3), 1.65 (2H, m, CH_2), 3.25 (2H, t, CH_2), 3.86 (2H, s, Ar- CH_2 -Ar), 4.10 (2H, t, CH_2), 7.05–7.42 (8H, m, Ar-H). Elemental analysis ($\text{C}_{41}\text{H}_{65}\text{N}_3\text{O}_4$): calcd: C 74.17, H 9.87, N 6.64, found: C 73.48, H 9.92, N 6.31. MS (LC-MS): m/z = 663.5 (M^+). GPC (THF): PDI = 1.00, M_n = 1368, M_w = 1376.

Compound B2. A solution of G1.5-C18 (3 g, 1.87 mmol) in dry THF (25 mL) was mixed with *n*-butylamine (0.14 g, 2.24 mmol) at 70 °C under dry nitrogen gas. The reaction mixture was stirred for 4 h and all of the G1.5-C18 was consumed, as monitored by IR spectra. B2 (2.71 g, 87%) was purified by precipitation from methanol as a light yellow powder. FT-IR

(KBr): 3360 cm^{-1} (NH), 1707 cm^{-1} [(NH)C=O]. ^1H NMR (chloroform- d): δ (ppm) = 0.85 (9H, t, CH_3), 1.22 (62H, m, CH_2), 1.52 (18H, s, CH_3), 1.58 (4H, t, CH_2), 1.62 (4H, m, CH_2), 2.70 (4H, t, CH_2), 3.25 (4H, t, CH_2), 3.85 (6H, s, Ar- CH_2 -Ar), 4.11 (4H, t, CH_2), 7.05–7.42 (24H, m, Ar-H). Elemental analysis ($\text{C}_{101}\text{H}_{148}\text{N}_{10}\text{O}_{11}$): calcd: C 71.60, H 8.80, N 8.27, found: C 72.08, H 8.77, N 8.02. MS (LC-MS): m/z = 1677.1 (M^+). GPC (THF): PDI = 1.01, M_n = 2093, M_w = 2115.

Compound B3. A solution of G2.5-C18 (4 g, 1.10 mmol) in dry THF (25 mL) was mixed with *n*-butylamine (0.08 g, 2.20 mmol) at 70 °C under dry nitrogen gas. The reaction mixture was stirred for 6 h and all of the G2.5-C18 was consumed, as monitored by IR spectra. B3 (3.1 g, 75%) was purified by precipitation from methanol as a light yellow powder. FT-IR (KBr): 3350 cm^{-1} (NH), 1707 cm^{-1} [(NH)C=O]. ^1H NMR (chloroform- d): δ (ppm) = 0.92 (15H, t, CH_3), 1.23 (122H, m, CH_2), 1.50 (42H, s, CH_3), 1.61 (10H, m, CH_2), 2.76 (12H, t, CH_2), 3.27 (14H, t, CH_2), 3.83 (14H, s, Ar- CH_2 -Ar), 4.13 (8H, t, CH_2), 6.95–7.54 (56H, m, Ar-H). Elemental analysis ($\text{C}_{221}\text{H}_{314}\text{N}_{24}\text{O}_{25}$): calcd: C 71.60, H 8.54, N 9.07, found: C 70.03, H 8.64, N 8.42. MS (MALDI-TOF): m/z = 3704.4 (M^+). PDI = 1.02, M_n = 3975, M_w = 4052.

Preparation of honeycomb-like polymeric film

Honeycomb-like polymeric films from the BF method were prepared according to the following procedure. First, a polymer containing a certain amount of dendrons was dissolved in CHCl_3 at various concentrations. Subsequently, the polymer solution was cast on a glass substrate under highly humid air (relative humidity, RH \sim 90%). The water droplets from the vapor condensed spontaneously on the surface of the polymer solution due to the decreased temperature caused by the evaporation of the solvent. The presence of dendrons prevented the water droplets from aggregating. These droplets were packed into a hexagonal array by a thermocapillary force as driven by gas flow and Marangoni convection.^{37–40} After complete evaporation of water and solvent, a honeycomb-like morphology was formed on the glass substrate.

Measurement

^1H NMR spectra were taken on a Bruker Avance-300 MHz FT-NMR spectrometer with chloroform- d and dimethyl sulfoxide- d_6 . Elemental analysis was performed on a Heraeus CHN-OS Rapid Analyzer. Infrared spectra were recorded to identify the chemical structure using a Jasco 4100 FT-IR Spectrophotometer with a Jasco ATR Pro 450-S accessory. Mass spectra were obtained using an LC/MS system including a Dynamax Model SD-200 solvent-delivery system (Rainin, Woburn, MA, USA) and a Hewlett-Packard (Palo Alto, CA, USA) HP5898 B quadrupole mass spectrometer equipped with an HP59987 A electrospray interface. Matrix-assisted laser desorption ionization with a time of flight (MALDI-TOF) mass spectra were recorded on a Voyager DE-PRO (Applied Biosystems, Houston, TX) equipped with a nitrogen laser (337 nm) operating in linear detection mode to generate positive ion spectra with dithranol as a matrix, dimethyl sulfoxide (DMSO) as a solvent and sodium

trifluoroacetate as an additive agent. Gel permeation chromatography (GPC) was performed using a Waters chromatography system, two Waters Styragel linear columns, and polystyrene as the standard. THF was used as the eluent at a flow rate of 0.84 mL min^{-1} at 40°C . Scanning electron microscopy (SEM) images were recorded using a Hitachi S-5200 field-emission scanning electron microscope after sputtering the films with a thin layer of Au/Pt alloy. Interfacial tensions of solutions were measured at 298 K using a KRÜSS Tensiometer K9 (ring method).

3. Results and discussion

Synthesis and characterization

In this study, a series of poly(urea/malonamide) dendrons were synthesized (Fig. 1). These dendrons of different generations exhibited hydrogen bond-rich linkages in the focal part, and alkyl chains in the periphery (–C18 or –C4).

With a dual-functional IDD as a building block, poly(urea/malonamide) dendrons were synthesized by a convergent approach,⁴¹ as shown in Scheme 1. *Via* this approach, one is able to control the low-number polymer growth each time. Both the isocyanate and the azetidine-2,4-dione group provided a fast and selective way of synthesizing the dendrons in mild conditions without resorting to traditional protection and activation chemistry.^{24,26}

G0.5-C4 was synthesized by the addition reaction between the isocyanate group of IDD and the hydroxyl group of *n*-butanol under mild conditions. Subsequently, G1.0-C4 was readily obtained through the ring-opening reaction of the azetidine-2,4-dione functional group of G0.5-C4 with the aliphatic primary amines of DETA. This azetidine-2,4-dione functional group reacts only with the aliphatic primary amines groups, but not with the secondary amine at the center of DETA or the hydroxyl group.^{24,30} G1.5-C4 was obtained by the addition reaction between the isocyanate of IDD and the secondary amine functional group located at the focal point of G1.0-C4. Finally,

a series of dendrons of various generations were achieved under mild conditions without the addition of catalysts by the sequential and alternative reactions of the IDD and DETA compounds. These poly(urea/malonamide) dendrons with long alkyl chains (G0.5-C18, G1.5-C18, and G2.5-C18) were synthesized in the same manner according to the previous study.^{24,30} To adjust the amphiphilicity, primary amine-containing reagents bearing various numbers of hydroxyl functional groups (–N(CH₂CH₂OH)₂, –CH₂CH₂OH, and –CH₂CH₂CH₂CH₃) were respectively reacted with the focal point *i.e.* azetidine-2,4-dione of G0.5-C18, G1.5-C18, and G2.5-C18 to form compounds of A, E, and B series (Scheme 2).

IR spectra of G0.5-C4, G1-C4, G1.5-C4, G2-C4 and G2.5-C4 are shown in Fig. S1.† The absorption peaks of 2260 cm^{-1} (N=C=O absorption of IDD) is absent in all spectra, indicating that the reaction of the highly reactive isocyanate group with active hydrogens was complete. ¹H NMR spectrum of G0.5-C4 exhibited chemical shifts at 3.90 (2H, s, Ar-CH₂-Ar) and 4.13 (2H, t, CH₂) (Fig. S2†). The ratio of the integrated areas conformed with the number of hydrogens. For G1.0-C4, the IR absorption peaks at 1857 cm^{-1} (C=O asymmetric stretching) and 1734 cm^{-1} (C=O symmetric stretching) of azetidine-2,4-dione disappeared and were displaced by the emergence of a new absorption peak at 1707 cm^{-1} (C=O stretching) of malonamide. ¹H NMR of spectrum of G1.0-C4 exhibited chemical shifts at 2.70 (4H, t, CH₂), 3.27 (4H, t, CH₂), 3.90 (4H, s, Ar-CH₂-Ar), 4.12 (4H, t, CH₂). The ratio of integrated areas conformed with the number of hydrogens. The analyses of G1.5-C4, G2.0-C4 and G2.5-C4 were also performed in the same manner. In addition, these well-defined dendritic polymer structures were determined by elemental analysis (EA), mass spectra (Mass) and gel permeation chromatography (GPC) as shown in Table 1. All these dendritic compounds exhibited monodisperse distribution (PDI < 1.01) as shown in Table 1.

The synthesis of amphiphilic dendrons (E series, for example) was traced by the IR spectra, as shown in Fig. S1.† The absorption peaks of azetidine-2,4-dione, 1854 cm^{-1} (C=O asymmetric stretching) and 1734 cm^{-1} (C=O symmetric stretching) of azetidine-2,4-dione disappeared completely, while the peaks at 1707 cm^{-1} (C=O stretching) of malonamide

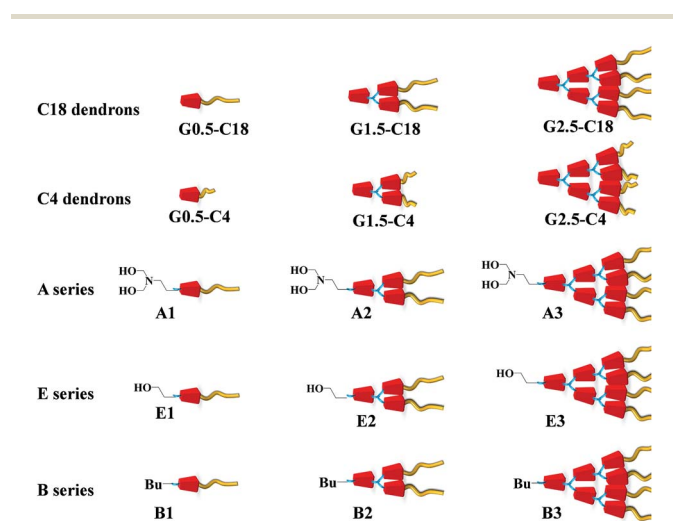


Fig. 1 Schematic drawings of dendritic poly(urea/malonamide) surfactants.

Table 1 Characteristics and polydispersities of poly(urea/malonamide) dendrons

Sample	Calcd M_n	M_n^a	M_w^b	M_n^b	PD ^b
G0.5-C4	394.2	394.1	517	514	1.00
G1.0-C4	891.5	891.6	943	933	1.01
G1.5-C4	1211.6	1211.5	1922	1911	1.01
G2.0-C4	2526.3	2526.1	2692	2665	1.01
G2.5-C4	2846.4	2846.2	3089	3066	1.01
E1	651.5	651.5	1452	1439	1.01
E2	1665.1	1666.9	2115	2093	1.01
E3	3692.4	3694.2	4334	4297	1.01
B1	663.5	663.5	1376	1368	1.00
B2	1677.1	1677.2	2115	2093	1.01
B3	3704.4	3704.2	4052	3975	1.02

^a Determined by ESI MS and MALDI-TOF MS. ^b Determined by GPC analysis in THF (calibration with polystyrene standards).

emerged. ^1H NMR spectrum exhibited chemical shifts at 2.70 (4H, t, CH_2), 3.27 (4H, t, CH_2), 3.90 (4H, s, Ar- CH_2 -Ar), 4.12 (4H, t, CH_2) (Fig. S2 †). The chemical structures of the resultant compounds were fully confirmed by FT-IR, ^1H NMR, elemental analysis (EA), and mass spectra (Mass). On the other hand, B series dendrons were synthesized in the same way as the E series. Detailed structural analyses and characterizations are shown in Fig. S1, S2 † and Table 1.

The solubility properties of these dendritic structures are shown in Table S1. † In particular, they all exhibited excellent solubility in CHCl_3 . Dendrons with butyl groups at the periphery (G0.5-C4, C1.5-C4 and G2.5-C4) possessed less hydrophobicity than did those with octadecyl groups (G0.5-C18, C1.5-C18 and G2.5-C18). The dendrons with peripheral octadecyl groups were soluble in toluene. In addition, G0.5-C4, C1.5-C4 and G2.5-C4 showed better solubility with polar protic solvents such as methanol and ethanol, implying that the dendritic structures with peripheral short alkyl chains (C4) preferred to dissolve in water instead of moving to the water-solution interface as a surfactant. On the other hand, G0.5-C18, C1.5-C18 and G2.5-C18 were totally insoluble in polar protic solvents. These findings indicate that the peripheral parts of the dendrons are responsible for the hydrophobicity of poly(urea/malonamide) dendritic compounds. Based on the above, the dendritic structures with peripheral long alkyl chains (C18) were chosen for a further role as surfactants. It is important to note that these chosen dendrons comprising a focal part featuring urea/malonamide functional groups and a peripheral part featuring long alkyl chains such as C18 have been proven to be effective surfactants for the breath figure process.^{31,32}

Furthermore, the moieties at the focal points could possibly be responsible for the adsorption onto the interface between water droplets and solution.¹⁵ Therefore, the right approach is to select a surfactant with an amphiphilic nature. With this in mind, the compounds in the A series would be a better choice for this purpose compared to those in the E and B series. Consequently, the A3 dendron with the highest hydrophilic and hydrophobic characteristics on the either end of molecules was first chosen to be the surfactant for the following investigations.

Morphologies

Dendrons as surfactants. We first used dendron A3 as an example to discuss the feasibility of the dendrons for preparing porous films. To prepare the film through the breath figure method, A3 was mixed with poly(D,L-lactide) (PLA) in chloroform. Fig. 2 shows the SEM images of the film surfaces prepared at RH = 95% with various dendron/PLA ratios in chloroform at 10 wt%. Without the surfactant in solution, the surface is basically flat, as shown in the pristine PLA sample (Fig. 2(a)). Well-organized honeycomb-like films were observed in the presence of dendritic surfactants for the dendron/PLA samples with weight ratios ranging from 1/99 to 100/0 (dendron/PLA). A small amount of dendritic surfactant is sufficient to create a honeycomb-like structure. Due to its amphiphilic nature, the surfactant can stabilize the water droplets condensed from the water vapor upon the quick evaporation of chloroform to

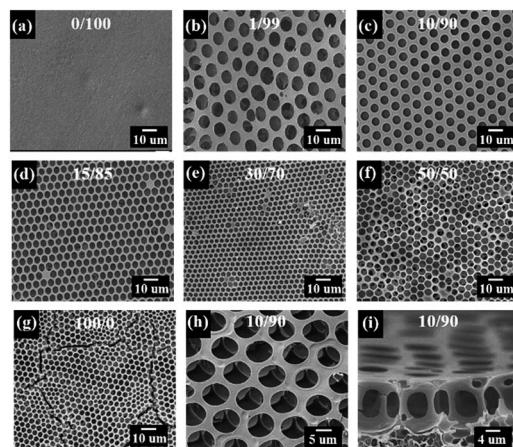


Fig. 2 SEM images of honeycomb-like films from the breath figure process (95% RH) for the samples with various A3/PLA ratios in chloroform (10 mg mL^{-1}): (a)–(g) top-view, (h) top-view with smaller features and (i) cross section of A3/PLA = 10/90.

prevent water droplets from merging on the surface. The uniform water droplets can then organize into hexagonally close-packed arrays once the number density of the droplets exceeds a threshold. These honeycomb polymeric films can be free-standing owing to the support of the polymer matrix. By the approach of blending dendritic surfactant and matrix polymer, hexagonal arrays could be obtained, which circumvents a complicated polymerization process that may result in low molecular weight and low grafting ratio due to the presence of bulky dendritic side-chains.^{31–33}

The pore size is highly dependent on the ratio of surfactant to polymer. Fig. 2(a)–(e) reveals that for the films with the dendron as the minor component (weight ratios of dendron/PLA up to 30/70), the higher the ratio of A3 dendron to PLA, the smaller the pore size of the honeycomb-like structure. This is because more surfactant molecules can adsorb onto the larger water-solution interfacial area and can thus stabilize smaller droplets that possess a higher surface area-to-volume ratio. The size dependence indicates that the dendritic surfactants are efficient in controlling the pore size during honeycomb formation by the BF method. For the films with the dendron as the major component (weight ratios of dendron/PLA higher than 50/50), the pores become less ordered, which may be due to a lack of sufficient support from the PLA as a matrix (Fig. 2(f)). The film with 100% dendrons even forms cracks on the surface, implying the necessity for a polymer matrix to create highly ordered honeycomb arrays as well as to provide film integrity (Fig. 2(g)). The surface roughness of the A3/PLA (10/90) sample with the smaller features is shown in Fig. 2(h). The surfaces of the roofs and cell bottoms were smooth at $2500\times$, indicating that no aggregation was present during the BF process. In addition, Fig. 2(i) displays the cross-sectional SEM image of the A3/PLA (10/90) sample, indicating that the height between the top thin layer and the second layer of the honeycomb-like polymer film was around $10 \mu\text{m}$.

The porous structure also depends on the solid content of the solution. Fig. 3 shows the SEM images of the films prepared from the solutions with a dendron/PLA weight ratio of 10/90 at various concentrations in chloroform. It is found that the solution with a concentration of 10 mg mL^{-1} can create the most ordered honeycomb arrays. The time period of solvent evaporation during the film formation varies with the solid content, which determines the amount of water condensed on the surface as well as the time at which the structure is frozen. Furthermore, the solid content also affects the fluidity of the solution during solvent evaporation and the film formation process. All the factors mentioned above may influence the quality of the honeycomb structures. There is thus an optimal concentration for the preparation of honeycomb-like arrays.

Generation of the surfactants. The porous morphologies also vary with the generation of the dendrons and the length of the alkyl chains in the peripheral part, as shown in Fig. 4 where the films were prepared from the sample with a dendron/PLA weight ratio of 10/90 in chloroform (10 mg mL^{-1}). Due to the cascade reaction of poly(urea/malonamide), the dendrons grow into a larger amphiphilic macromolecule with increasing generation of dendrons, and the numbers of repeat units in the focal part and the peripheral part increase accordingly. Fig. 4(a)–(c) show that for the dendrons with butyl groups in the peripheral part,

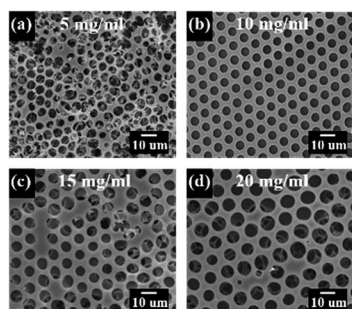


Fig. 3 SEM images of honeycomb-like films from the breath figure process (95% RH) for the sample (A3/PLA = 10/90) under various solution concentrations in chloroform ((a) 5, (b) 10, (c) 15 and (d) 20 mg mL^{-1}).

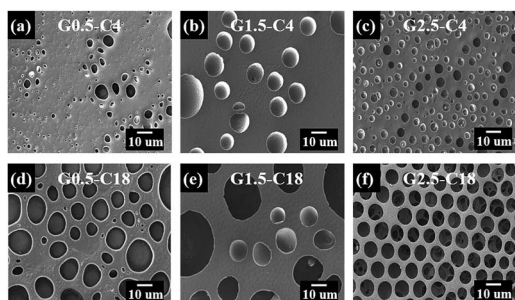


Fig. 4 SEM images of honeycomb-like films from the breath figure process (95% RH) for the PLA samples comprising dendrons with peripheral butyl and octadecyl groups ((a) G0.5-C4, (b) G1.5-C4, (c) G2.5-C4, (d) G0.5-C18, (e) G1.5-C18, and (f) G2.5-C18): dendrons/PLA = 10/90 in chloroform (10 mg mL^{-1}).

they hardly produce a well-organized morphology regardless of the dendron generation, which is attributed to two aspects: first, the dendrons prefer to be dissolved in water rather than move to the water–solution interface because of the short alkyl chains, which will be confirmed in the section of interfacial tension below, and, second, the short alkyl chains are unable to cause sufficient steric repulsion for the stabilization of the water droplets in solution. On the other hand, the dendrons with octadecyl groups in the peripheral part show a dependence of the morphologies on the dendron generation (Fig. 4(d)–(f)). G2.5-C18 dendrons as surfactants in the PLA polymer solution can create a hexagonal honeycomb array while the pores on the films with G0.5-C18 and G1.5-C18 are large and irregularly arranged. The results indicate that sufficiently large amphiphilic dendrons are crucial for fabricating a hexagonal array through the BF method. It is possible that the dendrons of higher generations, *i.e.* higher molecular weights, have a higher tendency to adsorb onto the interface between water droplets and solution due to the reduction in the miscibility of dendrons with both chloroform and water.

Focal point of the surfactants. In addition to the dendron generation and the chain length of the peripheral part, the moieties on the focal part of the dendrons also play an important role in the porous formation under the same BF condition. By a reaction between the azetidine-2,4-dione of the dendron and the primary amines of the desired reagents, the dendrons with different moieties at the focal point, including $-\text{N}(\text{CH}_2\text{CH}_2\text{OH})_2$, $-\text{CH}_2\text{CH}_2\text{OH}$, and $-\text{CH}_2\text{CH}_2\text{CH}_2\text{CH}_3$, were obtained. The films prepared from the solutions with a dendron/PLA weight ratio of 10/90 in chloroform (10 mg mL^{-1}) are compared in Fig. 5. It can be seen that the regularity of the porous structure depends significantly on the type of the functional groups at the focal point.

For the films comprising the modified G0.5-C18 series (A1, E1 and B1) with lower molecular weights, fractal bumps were found for the film with the A1 surfactant (bearing two hydroxyl

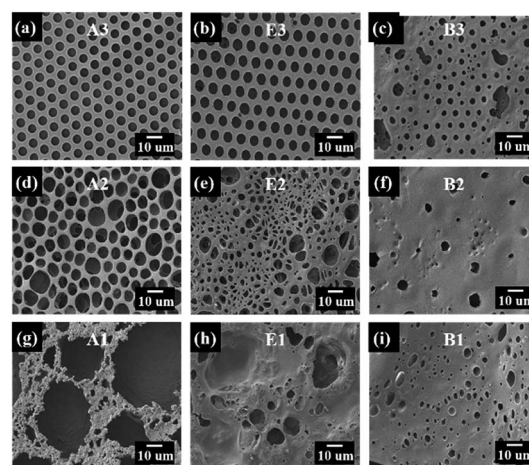


Fig. 5 SEM images of honeycomb-like films from the breath figure process (95% RH) for the PLA samples comprising dendrons with different focal parts: dendrons/PLA ((a) A3, (b) E3, (c) B3, (d) A2, (e) E2, (f) B2, (g) A1, (h) E1, and (i) B1) = 10/90 in chloroform (10 mg mL^{-1}).

groups), while irregular pores were observed for the films with E1 (bearing one hydroxyl group) or B1 (bearing butyl group). The water droplets are difficult to stabilize due to the low molecular weights of the modified G0.5-C18, even for A1 and E1 that are amphiphilic in nature. For the films comprising the modified G1.5-C18 series (A2, E2 and B2) that possess higher molecular weights, the morphology is dependent on the functional groups at the focal point under a similar BF process. A more ordered honeycomb array was obtained when the hydrophilicity increased in the focal part of the surfactant. As shown in the SEM images, the A2 surfactant stabilized more water droplets on the surface and prevented them from aggregating than E2 did. That is because A2 has a more distinct hydrophilic and hydrophobic moiety, so that it prefers to be located at the interface. B2 induced little irregular porous structure on the surface owing to its lack of amphiphilicity. For the films comprising the modified G2.5-C18 series (A3, E3 and B3), both A3 and E3 were able to create ordered honeycomb arrays on the films, while the pores on the film with B3 were disordered. These results demonstrate the importance of the hydrophilicity of the functional groups at the focal point in the formation of honeycomb-like arrays.

Interfacial tension

The stability of the water droplets lies in the adsorption of the dendritic surfactants onto the water–solution interface, and the driving force for the adsorption is to lower the interfacial tension. To make a quantitative analysis, the interfacial tensions between water and polymer solution with various types of dendrons (dendron/PLA = 10/90) in chloroform as a function of concentration were measured (Fig. 6). The interfacial tension at various solute concentrations (from 1 mg mL⁻¹ to high 100 mg mL⁻¹) was taken into account because during the BF process, the solvent evaporation would cause the concentration to increase and the interfacial tension might change accordingly.²²

For the pristine PLA solution, the interfacial tension between water and the solution remains almost constant as

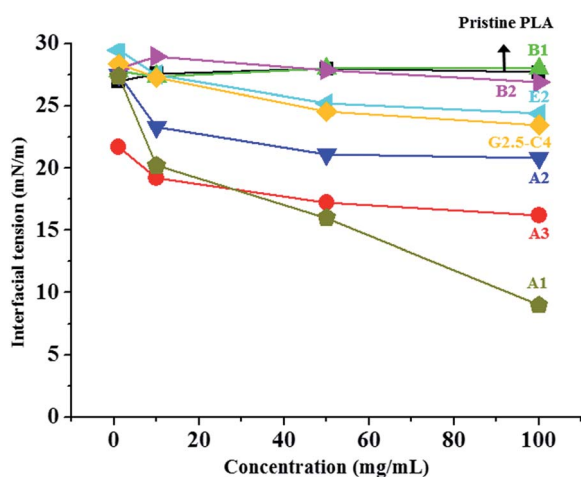


Fig. 6 Interfacial tension between water and polymer solution with various types of dendrons (dendron/PLA = 10/90) in chloroform as a function of concentration.

concentration varies, indicating that PLA doesn't prefer to gather at the interface, so that PLA alone has no significant effect on the interfacial tension. This result is consistent with the poor capability of pure PLA to form honeycomb pattern, as shown in Fig. 2(a). For the samples comprising the B dendron series, the interfacial tension is also nearly independent of concentration, also reflecting their poor ability to induce honeycomb patterns (Fig. 5(c), (f) and (i)).

In contrast, with the addition of A1 as surfactant, the interfacial tension largely decreases from ~ 27 mN m⁻¹ to ~ 10 mN m⁻¹, as the concentration increases from 1 to 100 mg mL⁻¹. Although the amphiphilic nature of A1 can effectively lower the interfacial tension between water and solution, the ability of A1 to induce a honeycomb structure is rather poor (Fig. 5(g)). This may be because the surfactant with a higher hydrophilic ratio allows A1 to diffuse to the water–air surface when water condenses, which in turn greatly lowers the surface tension of the water–air surface. Along with the low interfacial tension of the water–solution interface, as shown in Fig. 6, the spreading coefficient, *i.e.* the solution–air surface tension minus the sum of the water–solution interfacial tension and the water–air surface tension, may become positive, especially in the final stage of evaporation when the concentration increases to further reduce the water–solution interfacial tension. As a result, the condensed water prefers to form flat layers instead of water droplets for A1 solutions. For the solution with A3 as surfactant, the interfacial tension decreases sharply in the presence of a small amount of A3 (1 mg mL⁻¹) and then slowly decreases to 15 mN m⁻¹ with increasing concentration. The capability of A3 to create regular honeycomb arrays is contributed from the distinct amphiphilicity that allows A3 to adsorb onto the water–solution interface as well as the appropriate chemical architecture that creates balanced interfacial tensions among the three interfaces. Thus it is capable of maintaining water in droplet form without wetting; that is, there is a negative spreading coefficient in this system.²²

The trend of the interfacial tension curve of A2 is similar to that of A3, except that the interfacial tension is higher. This means that A2 as a surfactant can induce a honeycomb morphology but not as ordered as that of A3 (Fig. 5(a) and (d)). For E2 and G2.5-C4, the changes in the interfacial tension with concentration are similar, both showing a slight decrease as the concentration increases (Fig. 6). The surface morphologies of the films comprising E2 and G2.5-C4 look similarly disordered too (Fig. 4(c) and 5(e)), indicating that their tendency to adsorb onto the water–solution interface is poor and thus they are unable to efficiently stabilize the water droplets. These results suggest that to create ordered honeycomb structures, the surfactants should be able to locate at the water–solution interface to stabilize the water droplet, which in turn lowers the interfacial tension. However, the interfacial tension of the water–solution interface should not be lowered too much; otherwise the condensed water tends to wet the surface instead of forming droplets. The finding here is consistent with the conclusion reached by Shimomura *et al.*²²

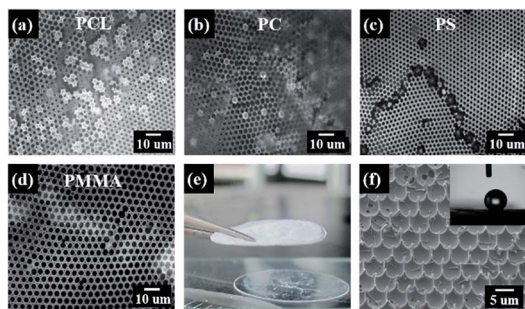


Fig. 7 Images of honeycomb-like surfaces obtained from the breath figure process (95% RH) based on a polymer solution comprising dendrons (A3/polymer = 10/90) in chloroform (10 mg mL^{-1}): (a) A3/PS, (b) A3/PCL, (c) A3/PC, (d) A3/PMMA from microscope, (e) photograph of free-standing A3/PMMA film, and (f) SEM image of superhydrophobic surface of the A3/PS honeycomb-like film after the peeling-off process.

Application

Honeycomb membranes can be fabricated from various polymers under the assistance of dendritic surfactants (A3) with a ratio of 10/90 (A3/polymer in chloroform at 10 wt%), as shown in Fig. 7. PS, PCL, PC and PMMA also exhibit well-ordered porous polymeric films through a similar BF process (Fig. 7(a)–(d)). Fig. 7(e) shows that the A3/PMMA film can be free-standing owing to the presence of a polymer matrix.

To achieve superhydrophobic behavior, the pincushion structures were fabricated by peeling off the top layer of the honeycomb polymeric film. With a glass transition temperature close to 100°C and good adhesion on the glass substrate, the polystyrene films with a honeycomb-like porous structure could be easily fabricated with a superhydrophobic surface ($\text{CA} \sim 152^\circ$), as shown in Fig. 7(f).

4. Conclusions

Through a convergent route, a series of dendritic poly(urea/malonamide) dendrons with well-defined structures were prepared. The amphiphilic nature of these dendrons was able to stabilize the water droplets condensed from the water vapor upon the quick evaporation of chloroform to prevent the coagulation of the water droplets on the surface and thus can be used as surfactants for fabricating polymer films with hexagonally close-packed arrays of pores through the breath figure method. It was found that the dendrons with one or two hydroxyl groups at the focal point and plenty of octadecyl groups in the periphery exhibited an amphiphilic characteristic, capable of creating well-balanced interfacial tensions among the water–solution, solution–air, and water–air interfaces that facilitate the formation of uniform and ordered arrays of water droplets, as evidenced by the measurements of the interfacial tensions between water and polymer solution with various types of dendrons as a function of concentration. Consequently, with the addition of a small amount of dendritic surfactants into polymers such as poly(D,L-lactide), polystyrene, polycarbonate, poly(methyl methacrylate), or polycaprolactone, a well-organized honeycomb-like surface

could be easily achieved after the evaporation of the solvent. With the support of the polymer matrices, these films were able to exhibit free-standing capacity as well as superhydrophobicity.

Acknowledgements

We thank Chung-Shan Institute of Technology and Ministry of Science and Technology of Taiwan for financial support.

References

- 1 G. Widawski, M. Rawiso and B. Francois, *Nature*, 1994, **369**, 387–389.
- 2 M. H. Stenzel, C. Barner-Kowollik and T. P. Davis, *J. Polym. Sci., Part A: Polym. Chem.*, 2006, **44**, 2363–2375.
- 3 U. H. F. Bunz, *Adv. Mater.*, 2006, **18**, 973–989.
- 4 A. Zhang, H. Bai and L. Li, *Chem. Rev.*, 2015, **115**, 9801–9868.
- 5 A. Z. Thong, D. S. Wei Lim, A. Ahsan, G. T. Wei Goh, J. Xu and J. M. Chin, *Chem. Sci.*, 2014, **5**, 1375–1382.
- 6 K. Manabe, S. Nishizawa and S. Shiratori, *ACS Appl. Mater. Interfaces*, 2013, **5**, 11900–11905.
- 7 M. S. Park and J. K. Kim, *Langmuir*, 2005, **21**, 11404–11408.
- 8 M.-J. Chang, Y. Ai, L. Zhang, F. Gao and H.-L. Zhang, *J. Mater. Chem.*, 2012, **22**, 7704–7707.
- 9 Y. Zhu, R. Sheng, T. Luo, H. Li, J. Sun, S. Chen, W. Sun and A. Cao, *ACS Appl. Mater. Interfaces*, 2011, **3**, 2487–2495.
- 10 P. S. Brown, E. L. Talbot, T. J. Wood, C. D. Bain and J. P. S. Badyal, *Langmuir*, 2012, **28**, 13712–13719.
- 11 C. Du, A. Zhang, H. Bai and L. Li, *ACS Macro Lett.*, 2013, **2**, 27–30.
- 12 H. Yabu, M. Tanaka, K. Ijiri and M. Shimomura, *Langmuir*, 2003, **19**, 6297–6300.
- 13 D. Fan, X. Xia, H. Ma, B. Du and Q. Wei, *J. Colloid Interface Sci.*, 2013, **402**, 146–150.
- 14 X. Jiang, T. Zhang, L. Xu, C. Wang, X. Zhou and N. Gu, *Langmuir*, 2011, **27**, 5410–5419.
- 15 A. S. De León, S. Malhotra, M. Molina, R. Haag, M. Calderón, J. Rodríguez-Hernández and A. Muñoz-Bonilla, *J. Colloid Interface Sci.*, 2015, **440**, 263–271.
- 16 F. Pilati, M. Montecchi, P. Fabbri, A. Synytska, M. Messori, M. Toselli, K. Grundke and D. Pospiech, *J. Colloid Interface Sci.*, 2007, **315**, 210–222.
- 17 Y. Tian, C. Dai, H. Ding, Q. Jiao, L. Wang, Y. Shi and B. Liu, *Polym. Int.*, 2007, **56**, 834–839.
- 18 M. Tanaka, K. Yoshizawa, A. Tsuruma, H. Sunami, S. Yamamoto and M. Shimomura, *Colloids Surf., A*, 2008, **313–314**, 515–519.
- 19 B. Yao, Q. Zhu, L. Yao and J. Hao, *Appl. Surf. Sci.*, 2015, **332**, 287–294.
- 20 A. S. Karikari, S. R. Williams, C. L. Heisey, A. M. Rawlett and T. E. Long, *Langmuir*, 2006, **22**, 9687–9693.
- 21 A. S. de León, A. del Campo, M. Fernández-García, J. Rodríguez-Hernández and A. Muñoz-Bonilla, *Langmuir*, 2014, **30**, 6134–6141.
- 22 Y. Fukuhira, H. Yabu, K. Ijiri and M. Shimomura, *Soft Matter*, 2009, **5**, 2037–2041.
- 23 D. A. Tomalia, *Prog. Polym. Sci.*, 2005, **30**, 294–324.

- 24 C. P. Chen, S. A. Dai, H. L. Chang, W. C. Su and R. J. Jeng, *J. Polym. Sci., Part A: Polym. Chem.*, 2005, **43**, 682–688.
- 25 C. P. Chen, S. A. Dai, H. L. Chang, W. C. Su, T. M. Wu and R. J. Jeng, *Polymer*, 2005, **46**, 11849–11857.
- 26 S. A. Dai, C. P. Chen, C. C. Lin, C. C. Chang, T. M. Wu, W. C. Su, H. L. Chang and R. J. Jeng, *Macromol. Mater. Eng.*, 2006, **291**, 395–404.
- 27 M. C. Kuo, S. M. Shau, J. M. Su, R. J. Jeng, T. Y. Juang and S. H. A. Dai, *Macromolecules*, 2012, **45**, 5358–5370.
- 28 S. M. Shau, C. C. Chang, C. H. Lo, Y. C. Chen, T. Y. Juang, S. H. A. Dai, R. H. Lee and R. J. Jeng, *ACS Appl. Mater. Interfaces*, 2012, **4**, 1897–1908.
- 29 Y. Y. Siao, S. M. Shau, W. H. Tsai, Y. C. Chen, T. H. Wu, J. J. Lin, T. M. Wu, R. H. Lee and R. J. Jeng, *Polym. Chem.*, 2013, **4**, 2747–2759.
- 30 S. A. Dai, T. Y. Juang, C. P. Chen, H. Y. Chang, W. J. Kuo, W. C. Su and R. J. Jeng, *J. Appl. Polym. Sci.*, 2007, **103**, 3591–3599.
- 31 W. H. Ting, C. C. Chen, S. A. Dai, S. Y. Suen, I. K. Yang, Y. L. Liu, F. M. C. Chen and R. J. Jeng, *J. Mater. Chem.*, 2009, **19**, 4819–4828.
- 32 C. C. Chang, T. Y. Juang, W. H. Ting, M. S. Lin, C. M. Yeh, S. A. Dai, S. Y. Suen, Y. L. Liu and R. J. Jeng, *Mater. Chem. Phys.*, 2011, **128**, 157–165.
- 33 Y. A. Su, W. F. Chen, T. Y. Juang, W. H. Ting, T. Y. Liu, C. F. Hsieh, S. H. A. Dai and R. J. Jeng, *Polymer*, 2014, **55**, 1481–1490.
- 34 H. Bai, C. Du, A. Zhang and L. Li, *Angew. Chem., Int. Ed.*, 2013, **52**, 12240–12255.
- 35 C.-P. Chen, S. A. Dai, H.-L. Chang, W.-C. Su, T.-M. Wu and R.-J. Jeng, *Polymer*, 2005, **46**, 11849–11857.
- 36 C.-C. Tsai, T.-Y. Juang, S. A. Dai, T.-M. Wu, W.-C. Su, Y.-L. Liu and R.-J. Jeng, *J. Mater. Chem.*, 2006, **16**, 2056–2063.
- 37 H. Ma, Y. Tian and X. Wang, *Polymer*, 2011, **52**, 489–496.
- 38 S. Xu, M. Li, Z. Mitov and E. Kumacheva, *Prog. Org. Coat.*, 2003, **48**, 227–235.
- 39 R. Dong, J. Yan, H. Ma, Y. Fang and J. Hao, *Langmuir*, 2011, **27**, 9052–9056.
- 40 H. Hu and R. G. Larson, *J. Phys. Chem. B*, 2006, **110**, 7090–7094.
- 41 S. M. Grayson and J. M. J. Fréchet, *Chem. Rev.*, 2001, **101**, 3819–3868.